Two-Dimensional Angle Estimation for Monostatic MIMO Radar Using Expanded PARAFAC Model

Dong-Mei Huang, Jian-Zhong Xu, and Ding Li
Information Department, Naval Command College, Nanjing, 210016, China
Email: {dm_naval, wfqsyyy, wfqsyy}@163.com

Abstract —In this research, we address the problem of Two-Dimensional (2D) angle estimation for monostatic Multiple-Input Multiple-Output (MIMO) radar. An expanded PARAFAC model is proposed to make full use of the Vandermonde-like structure of the data model, which expands the received data through unitary transformation and links the problem of 2D angle estimation to the PARAFAC model. Unlike the traditional estimation algorithms such as multiple signal classification (MUSIC) and estimation method of signal parameters via rotational invariance techniques (ESPRIT), the proposed algorithm does not require spectral peak searching nor eigenvalue decomposition of the received signal covariance matrix. Furthermore, our algorithm can achieve automatic pairing of 2D angles, and it has blind and robust characteristic, therefore the proposed algorithm has higher working efficiency. In addition, the proposed algorithm can detect more targets and has better estimation accuracy than ESPRIT algorithm and PARAFAC method. Extensive numerical experiments verify the effectiveness and improvement of our algorithm.

Index Terms—multiple-input multiple-output radar, angle estimation, PAFAFAC decomposition

I. INTRODUCTION

There is no doubt that Multiple-Input Multiple-Output (MIMO) radar will be a backbone to the future war. The concept of MIMO radar is that the radar system simultaneously transmits mutually orthogonal waveforms with multiple antennas and receive the reflected echoes with multiple antennas. The information of an individual transmitter-to-receiver path is separated by the matched filter at the receiving end. The virtual transmitter-to-receiver paths enable MIMO radar to achieve more degrees of freedom than the traditional phase-array radar [1]. Theoretical research indicates that MIMO radar has several built-in advantages in noise suppression, overcoming the fading effect, improving spatial resolution, enhancing parameter identifiability, etc. [2]-[4].

Direction-of-Arrival (DOA) estimation is a canonical problem in MIMO radar that has aroused extensive attention in the past decade. In [5] and [6], Capon and multiple signal classification (MUSIC) algorithms were introduced into angle estimation for MIMO radar, respectively, which estimate parameters via the spectral peak searching and suffer from high computational complexity. ESPRIT method, which is short for the estimation method of signal parameters via rotational invariance techniques, has been discussed in [7] and [8]. It utilizes the shift invariance property of the virtual array in MIMO radar for parameters estimation, and ESPRIT method does not require spectral peak searching. Generally speaking, the computational complexity of multiplying two complex numbers is much more than that of two real numbers. To reduce the computation load, the unitary transform based ESPRIT algorithm was proposed in [9] for target location in bistatic MIMO radar, which computing ESPRIT with real number and has estimation performance very close to that of the ESPRIT method. The parallel factor analysis (PARAFAC) method, sometimes also referred to as trilinear decomposition algorithm, was developed for angle estimation in [10]-[11], which stacked up the received data into higher-dimensional tensors model. Along with Trilinear Alternating Least Square (TALS) [12], the loading matrices could be estimated thus parameters were obtained. To support on-line applications, an adaptive PARAFAC algorithm has been presented in [13], which lower the complexity of the existing batch mode PARAFAC algorithms and has estimation performance very close to that of non-adaptive ones. The compressed PARAFAC model has been derived in [14], which fits a low-rank tensor model in the compressed domain and solves the inverse problem in the low-dimensional space. It has been applied in angle and Doppler frequency estimation for monostatic uniform linear arrays (ULA) configured MIMO radar [15]. The PARAFAC method may be considered as a generalization of the ESPRIT method while achieving more accurate performance [16].

The ULA configured MIMO radar only have the ability for one-dimensional (1D) angle estimation, for Two-Dimensional (2D) angle estimation, 2D array manifold is needed. Typical 2D arrays including octagon array [17], cross array [18], L-shape array [19] and rectangular array [20]. It has been proven that an L-shape array has better accuracy potential than the other

Manuscript received July 22, 2016; revised January 20, 2017.
This work was supported by the China NSF Grants (61071163 and 61471191), the Fundamental Research Funds for the Central Universities (NP2015504), Funding of Jiangsu Innovation Program for Graduate Education (KYLX_0277), and partly funded by the Priority Academic Program Development of Jiangsu Higher Education Institutions (PADA).
Corresponding author email: wfqsyyy@163.com.
doi:10.12720/jcm.12.1.32-39

manifolds [21]. Inspired by the expansion effect of the unitary transform [11], an improved PARAFAC algorithm is developed for 2D angle estimation in this study. The virtual received data is formed through unitary transform, 2D angle estimation is linked to the PARAFAC model. The expanded PARAFAC model increase the effective aperture of the radar system, therefore the proposed algorithm outperformed the conversional PARAFAC algorithm [18]. Furthermore, it does not require singular value decomposition of the received data and can obtain automatically paired 2D angle estimations in the MIMO radar. Finally, computation complexity is analyzed and Cramér-Rao Bound (CRB) for 2D angle estimation in MIMO radar is derived. Also, simulation results are given to illustrate the good estimation capability of the proposed algorithm for L-shape monostatic MIMO radar system.

The paper outline is as follows. The data model for the L-shape monostatic MIMO radar is presented in Section 2. The expanded PARAFAC algorithm is derived in Section 3. The performance and complexity of the proposed algorithm is discussed in Section 4. Simulation results are given in Section 5. We end the paper by a brief concluding in Section 6.

Notation, capital letters $\mathbf{X}$ and lower case $\boldsymbol{x}$ in bold denote, respectively, matrices and vectors. The superscript $(\mathbf{X})^T$, $(\mathbf{X})^H$, $(\mathbf{X})^{-1}$ and $(\mathbf{X})^\dagger$ represent the operations of transpose, Hermitian transpose, inverse and pseudo-inverse, respectively; The subscript $\|\mathbf{X}\|_F$ denote the Frobenius norm of $\mathbf{X}$; $\otimes$ stands for the Kronecker product; The Khatri-Rao product (column-wise Kronecker product) is denoted by $\odot$, i.e., $[\boldsymbol{a}_1,\boldsymbol{a}_2,\cdots,\boldsymbol{a}_K]\odot[\boldsymbol{b}_1,\boldsymbol{b}_2,\cdots,\boldsymbol{b}_K]=[\boldsymbol{a}_1\otimes\boldsymbol{b}_1,\boldsymbol{a}_2\otimes\boldsymbol{b}_2,\cdots,\boldsymbol{a}_K\otimes\boldsymbol{b}_K]$; The $M\times M$ identity matrix is denoted by $\mathbf{I}_M$, and the $M\times M$ inverse permutation matrix is denoted by $\mathbf{\Pi}_M$.

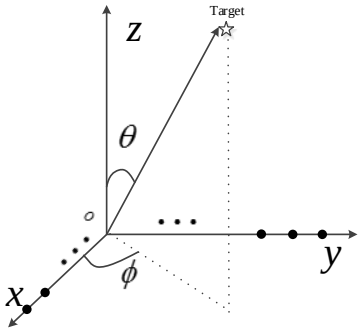

Fig. 1. monostatic L-shape MIMO radar

II. Data Model

We modeled a colocated MIMO radar system with L-shape configuration, as shown in Fig. 1. Suppose that there is an M -element transmitter located in the x -axis and an N -element receiver located in the y -axis, both of them are ULA with half-wavelength spacing, and the phase reference point of the transmitter and receiver are overlapped in the origin. Assume that K non-coherent targets appearing in the far-field of the antennas with the k -th target at azimuth angle φ_k and elevation angle θ_k . Additional assumptions are that the transmit antennas transmit narrowband orthogonal waveforms with the same carrier frequency. The echoes are collected at each receive antenna and passed through a set of matched filters for information extraction. The output of the matched filters in the n -th receiver takes the form [22]

$$\boldsymbol{r}_n(t)=\sum_{k=1}^{K}a_r^n(\theta_k,\varphi_k)\boldsymbol{a}_t(\theta_k,\varphi_k)s_k(t) \tag{1}$$

where

$$\boldsymbol{a}_r(\theta_k,\varphi_k)=\left[a_r^1(\theta_k,\varphi_k),\cdots,a_r^N(\theta_k,\varphi_k)\right]^T\in\mathbb{C}^{N\times 1}$$
$$\boldsymbol{a}_t(\theta_k,\varphi_k)=\left[a_t^1(\theta_k,\varphi_k),\cdots,a_t^M(\theta_k,\varphi_k)\right]^T\in\mathbb{C}^{M\times 1}$$

Respectively, denote the receive steering vector and the transmit steering vector for the k -th target, with the element $a_r^n(\theta_k,\varphi_k)=\exp\{-\mathrm{j}\pi(n-1)\sin\theta_k\cos\varphi_k\}$ $(n=1,2,\cdots,N)$, and the element $a_t^m(\theta_k,\varphi_k)=\exp\{-\mathrm{j}\pi(m-1)\sin\theta_k\sin\varphi_k\}$ $(m=1,2,\cdots,M)$. $s_k(t)=\alpha_k\exp\{j2\pi f_k t/f_s\}$ is the product of the radar cross section (RCS) α_k and the Doppler frequency shift f_k/f_s of the k -th target, f_k is the Doppler frequency, f_s is the pulse repeat frequency. Arrange $\boldsymbol{x}(t)=\left[\boldsymbol{r}_1(t),\boldsymbol{r}_2(t),\cdots,\boldsymbol{r}_N(t)\right]^T$, we have

$$\begin{aligned}\boldsymbol{x}(t)=\big[&\boldsymbol{a}_r(\theta_1,\varphi_1)\otimes\boldsymbol{a}_t(\theta_1,\varphi_1),\cdots,\\&\boldsymbol{a}_r(\theta_K,\varphi_K)\otimes\boldsymbol{a}_t(\theta_K,\varphi_K)\big]\boldsymbol{s}(t)\end{aligned} \tag{2}$$

where $\boldsymbol{s}(t)=\left[s_1(t),\cdots,s_K(t)\right]^T$ is a column vector. Let the transmit direction matrix $\mathbf{A}_T=\left[\boldsymbol{a}_t(\theta_1,\varphi_1),\cdots\boldsymbol{a}_t(\theta_K,\varphi_K)\right]\in\mathbb{C}^{M\times K}$, the receive direction matrix $\mathbf{A}_R=\left[\boldsymbol{a}_r(\theta_1,\varphi_1),\cdots\boldsymbol{a}_r(\theta_K,\varphi_K)\right]\in\mathbb{C}^{N\times K}$. Define the coefficient matrix as $\mathbf{S}=\left[\boldsymbol{s}(1),\cdots,\boldsymbol{s}(L)\right]^T\in C^{L\times K}$. Suppose that the directions of targets and the RCS coefficients are consist during L snapshots, hence the coefficient matrix has a Vandermonde-like structure without considering the RCSs:

$$\mathbf{S}=\begin{bmatrix}\alpha_1\exp\{j2\pi f_1/f_s\} & \cdots & \alpha_K\exp\{j2\pi f_K/f_s\}\\ \alpha_1\exp\{j4\pi f_1/f_s\} & \cdots & \alpha_K\exp\{j4\pi f_K/f_s\}\\ \vdots & \ddots & \vdots\\ \alpha_1\exp\{j2\pi Lf_1/f_s\} & \cdots & \alpha_K\exp\{j2\pi f_K L/f_s\}\end{bmatrix}$$

Neglecting the receive noise, the received data $\mathbf{X}=\left[\boldsymbol{x}(1),\boldsymbol{x}(2),\cdots,\boldsymbol{x}(L)\right]$ can be expressed as

$$\begin{aligned}\mathbf{X} &= \left[\boldsymbol{a}_r(\theta_1,\varphi_1)\otimes\boldsymbol{a}_t(\theta_1,\varphi_1),\cdots,\right.\\ &\quad \left.\boldsymbol{a}_r(\theta_K,\varphi_K)\otimes\boldsymbol{a}_t(\theta_K,\varphi_K)\right]\mathbf{S}^T \\ &= \left[\mathbf{A}_R \odot \mathbf{A}_T\right]\mathbf{S}^T = \mathbf{A}\mathbf{S}^T\end{aligned} \tag{3}$$

Here the direction matrix $\mathbf{A}=\left[\boldsymbol{a}(\theta_1,\varphi_1),\cdots\boldsymbol{a}(\theta_K,\varphi_K)\right] \in \mathbb{C}^{MN\times K}$, where the k th column $\boldsymbol{a}(\theta_k,\varphi_k)=\boldsymbol{a}_r(\theta_k,\varphi_k)\otimes\boldsymbol{a}_t(\theta_k,\varphi_k)$, which is known as the virtual array steering vector. The expression in (3) could be regarded as PARAFAC decomposition in matrix format, as a result, 2D angle estimation could be linked to the traditional PARAFAC model [11], [18]. However, the Vandermonde-like structure of the source matrix $\mathbf{S}$ is always ignored. Our aim is to increased estimation accuracy with the existing hardware architecture. For this purpose, a unitary transform based PARAFAC model is proposed in this research, which will be discussed in detail in the next section.

III. Improved PARAFAC Algorithm

A. Data Expansion Using Unitary Transformation

Employing the center of the ULA as the phase reference, the array manifold is conjugate centrosymmetric [23]. Given the receive array as an example, the central symmetry can be stated as $\mathbf{\Pi}_N\boldsymbol{a}_r(\theta_k,\varphi_k)=\boldsymbol{a}_r^*(\theta_k,\varphi_k)$. Define a simple unitary matrix

$$\mathbf{Q}_{2d=}\frac{1}{\sqrt{2}}\begin{bmatrix}\mathbf{I}_d & j\mathbf{I}_d\\ \mathbf{\Pi}_d & -j\mathbf{\Pi}_d\end{bmatrix}\in\mathbb{C}^{2d\times 2d} \tag{4}$$

if d is even, or

$$\mathbf{Q}_{2d+1}=\frac{1}{\sqrt{2}}\begin{bmatrix}\mathbf{I}_d & 0 & j\mathbf{I}_d\\ 0 & \sqrt{2} & 0\\ \mathbf{\Pi}_d & 0 & \mathbf{\Pi}_d\end{bmatrix}\in\mathbb{C}^{(2d+1)\times(2d+1)} \tag{5}$$

when d is odd. $\mathbf{Q}_N^H$ is a sparse unitary matrix which maps $\boldsymbol{a}_t(\theta_k,\varphi_k)$ onto an real-valued manifold. For example, if N is odd, we have

$$\begin{aligned}\boldsymbol{a}_r^Q(\mu_k)=\mathbf{Q}_N^H\boldsymbol{a}_r(\mu_k)=\sqrt{2}\exp\left\{\frac{(N-1)}{2}\pi\mu_k\right\}\cdot\left[\cos\left\{\left(\frac{N-1}{2}\right)\pi\mu_k\right\},\right.\\ \left.\cdots,\cos\{\pi\mu_k\},\frac{1}{\sqrt{2}},\sin\left\{\left(\frac{N-1}{2}\right)\pi\mu_k\right\},\cdots\sin\{\pi\mu_k\}\right]^T\end{aligned}$$

where $\mu_k=\sin\theta_k\cos\varphi_k$. Obviously, the column vector $\boldsymbol{a}_r^Q(\mu_k)$ can be expressed as the product of a complex value and a real-valued vector. Let $\mathbf{Q}=\mathbf{Q}_N\otimes\mathbf{I}_M$, we therefore have

$$\mathbf{Q}^H\boldsymbol{a}(\mu_k)=\left(\mathbf{Q}_N^H\boldsymbol{a}_r(\mu_k)\right)\otimes\boldsymbol{a}_t(\mu_k)=\boldsymbol{a}_r^Q(\mu_k)\otimes\boldsymbol{a}_t(\mu_k) \tag{6}$$

Define the transformed direction matrix $\mathbf{A}_Q$ as $\mathbf{A}_Q=\mathbf{Q}^H\mathbf{A}$. According to(6), we obtain $\mathbf{A}_Q=\mathbf{A}_R^Q\odot\mathbf{A}_T$ with $\mathbf{A}_R^Q=\mathbf{Q}_N^H\mathbf{A}_R$. The uncorrupted signals in(3) can be transformed into

$$\mathbf{X}_Q=\mathbf{Q}^H\mathbf{X}=\mathbf{Q}^H\mathbf{A}\mathbf{S}^T=\mathbf{A}_Q\mathbf{S}^T \tag{7}$$

On the other hand, due to the Vandermonde-like structure on $\mathbf{S}$, we have $\mathbf{S}^H\mathbf{\Pi}_L=\mathbf{\Lambda}\mathbf{S}^T$, where $\mathbf{\Lambda}=diag(\beta_1,\beta_2,\cdots,\beta_K)$ is a diagonal matrix with the elements $\beta_k=\exp\{-j2\pi f_k(L+1)/f_s\}$, $(k=1,\cdots,K)$. Notice that the source matrix $\mathbf{S}$ has a similar central symmetry to $\mathbf{A}_R$, another data matrix can be built

$$\mathbf{X}_L=\mathbf{X}_Q^*\mathbf{\Pi}_L=\mathbf{A}_Q^*\mathbf{\Lambda}\mathbf{S}^T=\mathbf{A}_L\mathbf{S}^T \tag{8}$$

one can easily find that $\mathbf{A}_L=\left[\mathbf{A}_R'\odot\mathbf{A}_T\right]$ with $\mathbf{A}_R'=\mathbf{A}_R^Q\mathbf{\Lambda}^*$. Without additive noise, the expanded data matrix is formed as following

$$\mathbf{X}_E=\begin{bmatrix}\mathbf{X}_Q\\ \mathbf{X}_L\end{bmatrix}=\begin{bmatrix}\mathbf{A}_R^Q\odot\mathbf{A}_T\\ \mathbf{A}_R'\odot\mathbf{A}_T\end{bmatrix}\mathbf{S}^T=\left[\mathbf{A}_E\odot\mathbf{A}_T\right]\mathbf{S}^T \tag{9}$$

where $\mathbf{A}_E=\begin{bmatrix}\mathbf{A}_R^Q\\ \mathbf{A}_R'\end{bmatrix}\in\mathbb{C}^{2N\times K}$. The expression in (9) could also be counted as expanded PARAFAC decomposition in matrix format, which can be expressed in detail

$$\mathbf{X}_E=[\mathbf{A}_E\odot\mathbf{A}_T]\mathbf{S}^T=\begin{bmatrix}\mathbf{X}_1\\ \mathbf{X}_2\\ \vdots\\ \mathbf{X}_{2N}\end{bmatrix}=\begin{bmatrix}\mathbf{A}_T D_1(\mathbf{A}_E)\\ \mathbf{A}_T D_2(\mathbf{A}_E)\\ \vdots\\ \mathbf{A}_T D_{2N}(\mathbf{A}_E)\end{bmatrix}\mathbf{S}^T \tag{10}$$

where $D_n(\mathbf{A}_R)$ denotes the operations of rearranging the n-th row of $\mathbf{A}_R^E$ into a diagonal matrix. The n-th slice $\mathbf{X}_n$ of $\mathbf{X}_E$ is given by $\mathbf{X}_n=\mathbf{A}_T D_n\left(\mathbf{A}_R^E\right)\mathbf{S}^T$ $(n=1,2,\cdots,2N)$. Equation (10) shows that expanded PARAFAC model essentially doubles the number of available measurements from MN to $2MN$. Consequently, increased estimation accuracy can be achieved by the expanded PARAFAC model. PARAFAC decomposition could be also expressed in scalar format

$$\begin{aligned}&x_{m,n,l}=\sum_{k=1}^{K}\mathbf{A}_T(m,k)\mathbf{A}_R^E(n,k)\mathbf{S}(l,k)\\ &(m=1,2,\cdots,M;n=1,2,\cdots,2N;l=1,2,\cdots,L)\end{aligned} \tag{11}$$

The model in (11), which rearranged the data from the array antennas into a cube, can be regarded as the trilinear slice model. It depicts the echo form the perspective of three different diversities, as shown in Fig. 2. The matrix $\mathbf{X}_n$ can be deem as slicing the cube data into successions of slices along the receive antenna direction. Due to the

symmetry of the parallel factor model, two more matrices can be constructed

$$\mathbf{Y}=\begin{bmatrix}\mathbf{Y}_1\\ \mathbf{Y}_2\\ \vdots\\ \mathbf{Y}_M\end{bmatrix}=\begin{bmatrix}\mathbf{S}D_1(\mathbf{A}_T)\\ \mathbf{S}D_2(\mathbf{A}_T)\\ \vdots\\ \mathbf{S}D_M(\mathbf{A}_T)\end{bmatrix}\mathbf{A}_E^T=[\mathbf{A}_T\odot\mathbf{S}]\mathbf{A}_E^T \quad (12)$$

and

$$\mathbf{Z}=\begin{bmatrix}\mathbf{Z}_1\\ \mathbf{Z}_2\\ \vdots\\ \mathbf{Z}_L\end{bmatrix}=\begin{bmatrix}\mathbf{A}_E D_1(\mathbf{S})\\ \mathbf{A}_E D_2(\mathbf{S})\\ \vdots\\ \mathbf{A}_E D_L(\mathbf{S})\end{bmatrix}\mathbf{A}_R^T=[\mathbf{S}\odot\mathbf{A}_E]\mathbf{A}_T^T. \quad (13)$$

where the slices $\mathbf{Y}_m=\mathbf{S}D_m(\mathbf{A}_T)\mathbf{A}_E^T$ $(m=1,2,\cdots,M)$ and $\mathbf{Z}_l=\mathbf{A}_E D_l(\mathbf{S})\mathbf{A}_T^T$ $l=1,2,\cdots,L$. The data matrices $\mathbf{Y}$ and $\mathbf{Z}$ can be interpreted as slicing the cube along the transmit antenna array direction the snapshot direction, respectively.

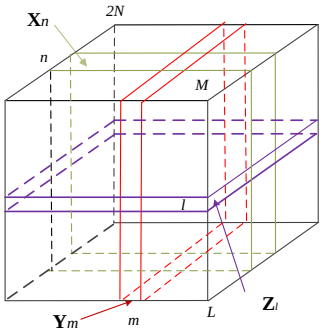

Fig. 2. Trilinear model

B. Trilinear Alternate Least Squares (TALS)

TALS is an effective algorithm to solve the PARAFAC model. The essence of TALS can be described as the following steps: **(a)** Fitting one of the slicing matrices $\mathbf{X}$, $\mathbf{Y}$ or $\mathbf{Z}$ using Least Squares (LS) method, where the remaining two matrices are previously obtained, **(b)** Fitting the other two matrices in a similar way, and **(c)** Repeat (a) and (b) until LS cost function convergence. The details of solving the expanded PARAFAC model with TALS algorithm is described as follows.

Consider the situation where noise is present, according to(10), the LS fitting of $\mathbf{X}_E$ is

$$f_{\tilde{\mathbf{X}}}=\min_{\mathbf{A}_E,\mathbf{B},\mathbf{A}_T^T}\left\|\tilde{\mathbf{X}}-[\mathbf{A}_E\odot\mathbf{A}_T]\mathbf{S}^T\right\|_F \quad (14)$$

where $\tilde{\mathbf{X}}$ represents the noisy $\mathbf{X}_E$. Therefore, the LS estimation for $\mathbf{S}$ is

$$\hat{\mathbf{S}}^T=\left[\hat{\mathbf{A}}_E\odot\hat{\mathbf{A}}_T\right]^{\dagger}\tilde{\mathbf{X}} \quad (15)$$

with $\hat{\mathbf{A}}_E$ and $\hat{\mathbf{A}}_T$ denote the estimated $\mathbf{A}_E$ and $\mathbf{A}_T$ in the last iteration. Similarly, the LS fitting of $\tilde{\mathbf{Y}}$ is $f_{\tilde{\mathbf{Y}}}=\min_{\hat{\mathbf{A}}_E,\mathbf{B},\hat{\mathbf{A}}_T^T}\left\|\tilde{\mathbf{Y}}-[\mathbf{A}_T\odot\mathbf{S}]\mathbf{A}_E^T\right\|_F$ where $\tilde{\mathbf{Y}}$ denotes the noisy $\mathbf{Y}$. The LS update for $\mathbf{A}_E$ is

$$\hat{\mathbf{A}}_E^T=\left[\hat{\mathbf{A}}_T\odot\hat{\mathbf{S}}\right]^{\dagger}\tilde{\mathbf{Y}} \quad (16)$$

where $\hat{\mathbf{A}}_T$ and $\hat{\mathbf{S}}$ are previously obtained. Finally, the LS fitting of $\tilde{\mathbf{Z}}$ is $f_{\tilde{Z}}=\min_{\mathbf{A}_R,\mathbf{S},\mathbf{A}_T^T}\left\|\tilde{\mathbf{Z}}-[\mathbf{S}\odot\mathbf{A}_E]\mathbf{A}_T^T\right\|_F$ and the LS update for $\mathbf{A}_T$ is

$$\hat{\mathbf{A}}_T^T=\left[\hat{\mathbf{S}}\odot\hat{\mathbf{A}}_E\right]^{\dagger}\tilde{\mathbf{Z}} \quad (17)$$

where $\hat{\mathbf{S}}$ and $\hat{\mathbf{A}}_E$ represent the previously estimated $\hat{\mathbf{S}}$ and $\mathbf{A}_E$, respectively.

C. Angle Estimation

The uniqueness property under mild conditions is a key feature of PARAFAC decomposition. Theorem 1 [24] gives the identifiablitity of the expanded PARAFAC model.

Theorem 1: $\mathbf{X}_n=\mathbf{A}_T D_n(\mathbf{A}_E)\mathbf{S}^T$, $(n=1,2,\cdots,2N)$, where $\mathbf{A}_T\in\mathbb{C}^{M\times K}$, $\mathbf{A}_E\in\mathbb{C}^{2N\times K}$, $\mathbf{S}\in\mathbb{C}^{L\times K}$. Consider that all the matrices are full k-rank [25], if the parameter identifiability satisfies

$$k_{\mathbf{A}_T}+k_{\mathbf{A}_E}+k_{\mathbf{S}}\geq 2K+2 \quad (18)$$

then $\mathbf{A}_T$, $\mathbf{A}_E$ and $\mathbf{S}$ are unique up to permutation and scaling of columns, where $k_{\mathbf{A}_T}$, $k_{\mathbf{A}_E}$ and $k_{\mathbf{S}}$ denote the k-rank of $\mathbf{A}_T$, $\mathbf{A}_E$ and $\mathbf{S}$, respectively. The estimated matrices $\hat{\mathbf{A}}_T$, $\hat{\mathbf{A}}_E$ and $\hat{\mathbf{S}}$ satisfy $\hat{\mathbf{A}}_T=\mathbf{A}_T\mathbf{\Pi}\mathbf{\Delta}_1+\mathbf{N}_1$, $\hat{\mathbf{A}}_E=\mathbf{A}_E\mathbf{\Pi}\mathbf{\Delta}_2+\mathbf{N}_2$ and $\hat{\mathbf{S}}=\mathbf{S}\mathbf{\Pi}\mathbf{\Delta}_3+\mathbf{N}_3$, where $\mathbf{\Pi}$ is a permutation matrix, $\mathbf{N}_1$, $\mathbf{N}_2$ and $\mathbf{N}_3$ represent the corresponding estimation error, and $\mathbf{\Delta}_1$, $\mathbf{\Delta}_2$ and $\mathbf{\Delta}_3$ stand for the diagonal scaling matrices satisfying $\mathbf{\Delta}_1\mathbf{\Delta}_2\mathbf{\Delta}_3=\mathbf{I}_K$.

Once TALS is accomplished, the estimated direction matrices $\mathbf{A}_E$ and $\mathbf{A}_T$ could be obtained. Since the phase of the columns in $\mathbf{A}_E$ and $\mathbf{A}_T$ have linear characteristics, so the LS method is reused for 2D angle estimation. The estimated transmit vector $\boldsymbol{a}_t(\theta_k,\varphi_k)$ was firstly normalized to the reference phase center. Let

$$\boldsymbol{h}_{k,1}=-angle\left(\hat{\boldsymbol{a}}_t(\theta_k,\varphi_k)\right) \quad (19)$$

where the operation $angle\left(\hat{\boldsymbol{a}}_t(\theta_k,\varphi_k)\right)$ is to get the phase of $\hat{\boldsymbol{a}}_t(\theta_k,\varphi_k)$. We construct the following matrix and vector

$$\mathbf{P}_1=\begin{bmatrix}1 & 1 & \cdots & 1\\ 0 & \pi & \cdots & (M-1)\pi\end{bmatrix}^T\in\mathbb{R}^{M\times 2},\quad \boldsymbol{u}_k=\begin{bmatrix}u_{k,1}\\ u_{k,2}\end{bmatrix} \quad (20)$$

Furthermore, the LS solution to $\boldsymbol{u}_k$ is

$$\boldsymbol{u}_k = \mathbf{P}_1^{\dagger}\boldsymbol{h}_{k,1} \tag{21}$$

One can easily find that $u_{k,2}$ is the LS estimation to $\sin\theta_k \cos\varphi_k$. Similarity, define

$$\boldsymbol{h}_{k,2} = -angle\left(\hat{\boldsymbol{a}}_e\left(\theta_k,\varphi_k\right)\right) \tag{22}$$

and construct

$$\mathbf{P}_2 = \begin{bmatrix} 0 & \cdots & 0 & 1 & \cdots & 1 \\ 0 & \cdots & (N-1)\pi & 0 & -\pi & -(N-1)\pi \end{bmatrix}, \boldsymbol{v}_k = \begin{bmatrix} v_{k,1} \\ v_{k,2} \end{bmatrix} \tag{23}$$

Next, we got the LS solution to $\boldsymbol{v}_k$

$$\boldsymbol{v}_k = \mathbf{P}_2^{\dagger}\boldsymbol{h}_{k,2} \tag{24}$$

One can easily find that $v_{k,2}$ is the LS estimation to $\sin\theta_k \sin\varphi_k$. The azimuth angle and elevation angle for the k-th target can be paired automatically through the following formula

$$\begin{cases} \theta_k = \arcsin\left(\sqrt{u_{k,2}+v_{k,2}}\right) \\ \varphi_k = \arctan\left(v_{k,2} \big/ u_{k,2}\right) \end{cases} \tag{25}$$

IV. Algorithm Analysis

A. Identifiablitity

The formulation in(18) provides an upper bound on the identifiablitity of the proposed PARAFAC algorithm. Generally, we have $k_{\mathbf{A}_T} = M$, $k_{\mathbf{A}_E} = 2N$ and $k_{\mathbf{S}} = \min(K,L)$ in the trilinear model established in this study. When $K \le L$, the inequality in (18) can be rewritten as $M+2N-2 \ge K$, which implies the maximum number of targets that the proposed algorithm can identify is $M+2N-2$, while the maximum number of targets that the traditional PARAFAC algorithm can detect is $M+N-2$ [10]. Under the condition of $K > L$, the proposed algorithm is effective when $K \le (M+2N+L-2)/2$, while the conditional PARAFAC algorithm is effective when $K \le (M+N+L-2)/2$, therefore, the proposed algorithm could achieve better estimation accuracy under the same conditions.

B. Computation Complexity

Traditional Capon and MUSIC algorithm requires 2D peak searching in a higher dimensional space, which brings very heavy complexity. The computation complexity of the traditional ESPRIT algorithm is $\mathrm{O}\left(M^2N^2L+M^3+N^3+K^3\right)$, complexity in each TALS iteration of the traditional PARAFAC algorithm is $\mathrm{O}\left(MNLK+K^3\right)$, and the proposed MCS algorithm needs $\mathrm{O}\left(2MNLK+K^3\right)$ calculations per TALS iteration, and algorithm convergence with only a few iterations. It is obvious that the computation complexity of the proposed algorithm is between the ESPRIT method and traditional PARAFAC algorithm.

C. Cramér-Rao Bound (CRB)

In this subsection, we derive CRB of 2D angle estimation in a monostatic MIMO radar. In particular, it provides an asymptotic lower bound on the 2D angle estimators. We assume that the signal $\mathbf{s}(t)$ and the noise variance σ^2 are deterministic, and then estimation parameter vector is expressed as

$$\boldsymbol{\zeta} = \left[\theta_1,\cdots,\theta_K,\varphi_1,\cdots\varphi_k\right]^T \tag{26}$$

Collect L snapshots and form the data matrix $\mathbf{X} = \left[\boldsymbol{x}(1)^T,\boldsymbol{x}(2)^T,\cdots,\boldsymbol{x}(L)^T\right]$. The mean $\boldsymbol{\mu}$ and the covariance matrix $\boldsymbol{\Gamma}$ of $\mathbf{X}$ are

$$\boldsymbol{\mu} = \begin{bmatrix} \mathbf{A}\boldsymbol{s}(1) \\ \vdots \\ \mathbf{A}\boldsymbol{s}(L) \end{bmatrix}, \quad \boldsymbol{\Gamma} = \begin{bmatrix} \sigma^2\mathbf{I}_{MN} & & 0 \\ & \ddots & \\ 0 & & \sigma^2\mathbf{I}_{MN} \end{bmatrix} \tag{27}$$

From [26], we know that the (i,j) element of the CRB matrix ($\mathbf{P}_{cr}$) can be expressed as

$$\left[\mathbf{P}_{cr}^{-1}\right]_{ij} = tr\left[\boldsymbol{\Gamma}^{-1}\boldsymbol{\Gamma}_i'\boldsymbol{\Gamma}^{-1}\boldsymbol{\Gamma}_j'\right] + 2\,\mathrm{Re}\left[\boldsymbol{\mu}_i'^H\boldsymbol{\Gamma}^{-1}\boldsymbol{\mu}_j'\right] \tag{28}$$

where $\boldsymbol{\Gamma}_i'$ and $\boldsymbol{\mu}_i'$ are the derivative of $\boldsymbol{\Gamma}$ and $\boldsymbol{\mu}$ on the ith element of $\boldsymbol{\zeta}$, respectively. Since the covariance matrix is just related to σ^2, the first part of (28) can be ignored. Then

$$\left[\mathbf{P}_{cr}^{-1}\right]_{ij} = 2\,\mathrm{Re}\left[\boldsymbol{\mu}_i'^H\boldsymbol{\Gamma}^{-1}\boldsymbol{\mu}_j'\right] \tag{29}$$

Define $\boldsymbol{a}_k = \boldsymbol{a}_r(\theta_k,\varphi_k)\otimes\boldsymbol{a}_t(\theta_k,\varphi_k)$, and we have

$$\frac{\partial\boldsymbol{\mu}_k}{\theta_k} = \begin{bmatrix} \dfrac{\partial\boldsymbol{a}_k}{\partial\theta_k}s_k(1) \\ \vdots \\ \dfrac{\partial\boldsymbol{a}_k}{\partial\theta_k}s_k(L) \end{bmatrix} = \boldsymbol{s}_k\otimes\boldsymbol{d}_k, \quad k=1,...,K \tag{30}$$

$$\frac{\partial\boldsymbol{\mu}_k}{\varphi_k} = \begin{bmatrix} \dfrac{\partial\boldsymbol{a}_k}{\partial\varphi_k}s_k(1) \\ \vdots \\ \dfrac{\partial\boldsymbol{a}_k}{\partial\varphi_k}s_k(L) \end{bmatrix} = \boldsymbol{s}_k\otimes\boldsymbol{f}_k, \quad k=1,...,K \tag{31}$$

where $\boldsymbol{d}_k = \dfrac{\partial\boldsymbol{a}_k}{\partial\theta_k}$, $\boldsymbol{f}_k = \dfrac{\partial\boldsymbol{a}_k}{\partial\varphi_k}$. $\boldsymbol{s}_k = \left[s_k(1),\cdots,s_k(L)\right]^T$ with $s_k(l)$ $(l=1,\cdots,L)$ denotes the kth element of $\mathbf{s}(l)$. Define the following matrix

$$\boldsymbol{\Delta} \triangleq \left[\boldsymbol{s}_1 \otimes \boldsymbol{d}_1, \cdots, \boldsymbol{s}_K \otimes \boldsymbol{d}_K, \boldsymbol{s}_1 \otimes \boldsymbol{f}_1, \cdots, \boldsymbol{s}_K \otimes \boldsymbol{f}_K\right] \quad (32)$$

Therefore we have $\frac{\partial \boldsymbol{\mu}}{\partial \boldsymbol{\zeta}^T} = \boldsymbol{\Delta}$, and

$$2\,\mathrm{Re}\left\{\frac{\partial \boldsymbol{\mu}^*}{\partial \boldsymbol{\zeta}} \boldsymbol{\Gamma}^{-1} \frac{\partial \boldsymbol{\mu}}{\partial \boldsymbol{\zeta}^T}\right\} = \frac{2}{\sigma^2}\mathrm{Re}\left\{\boldsymbol{\Delta}^H \boldsymbol{\Delta}\right\} \quad (33)$$

Thus the CRB for the 2D angle estimation error in MIMO radar is

$$CRB = \frac{\sigma^2}{2}\left(\mathrm{Re}\left(\mathbf{D}^H \mathbf{D}\right)\right)^{-1} \quad (34)$$

where $\mathbf{D} = \left[\mathbf{D} \otimes \mathbf{S}, \mathbf{F} \otimes \mathbf{S}\right]$, among which $\mathbf{D} = [\boldsymbol{d}_1, ..., \boldsymbol{d}_K]$, $\mathbf{F} = [\boldsymbol{f}_1, ..., \boldsymbol{f}_K]$.

V. Simulation Results

To evaluate the performance of the proposed 2D angle estimation algorithm, 1000 Monte Carlo trials are taken. The signal-to-noise in the simulation is defined by $\mathrm{SNR} = 10\log_{10}\left\|\mathbf{X}_E\right\|_F^2 \Big/ \left\|\mathbf{X}_E - \tilde{\mathbf{X}}\right\|_F^2$ [dB]. The root mean squared error (RMSE) is used for performance assessment, which is defined as follows

$$RMSE = \frac{1}{K}\sum_{k=1}^{K}\sqrt{\frac{1}{1000}\sum_{i=1}^{1000}\left\{\left(\hat{\theta}_{i,k} - \theta_k\right)^2 + \left(\hat{\varphi}_{i,k} - \varphi_k\right)^2\right\}}$$

where $\hat{\theta}_{i,k}$ and $\hat{\varphi}_{i,k}$ denote the estimation of elevation and azimuth angle of the k-th target in the i-th Monte Carlo trial. In the simulation, M, N and L denote the number of the transmit elements, receive elements and snapshots. We consider that there are $K = 3$ targets located at angles $(\theta_1, \varphi_1) = (10^\circ, 15^\circ)$, $(\theta_2, \varphi_2) = (20^\circ, 25^\circ)$ and $(\theta_3, \varphi_3) = (30^\circ, 35^\circ)$.

Fig. 3 present the 2D-DOA estimation results of our algorithm with SNR = 5dB. Parameters are set to $M = N = 8$ and $L = 40$, respectively. As seen in this figure, our algorithm is able to estimate azimuth angle and elevation angle for monostatic L-shape MIMO radar.

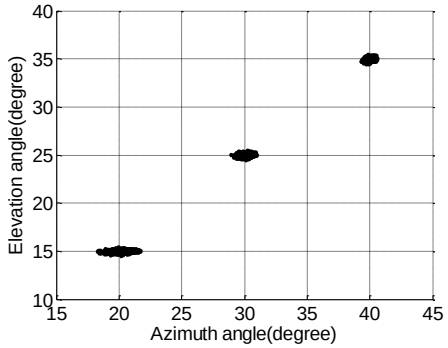

Fig. 3. Scatter results with SNR=5dB.

Fig. 4 depicts the performance comparison of our algorithm, the conventional ESPRIT algorithm, the Unitary-ESPRIT algorithm, the traditional PARAFAC algorithm and the CRB with $M = N = 8$ and $L = 40$. According to Fig. 4, the Unitary-ESPRIT algorithm has estimation performance very close to that of the ESPRIT method. Besides, all algorithms would achieve better RMSE performance with the growing SNR, and our algorithm outperform the other algorithms with the same SNR, especially in the condition of low SNR. Fig. 5 illustrate that the RMSE comparison of the above algorithms with different snapshots number with $M = N = 8$ and SNR=0dB. All algorithms exhibit an increasing RMSE trend with the increase in the number of snapshots, and it is obvious that our algorithm has much better 2D angle estimation than ESPRIT and the traditional PARAFAC algorithm.

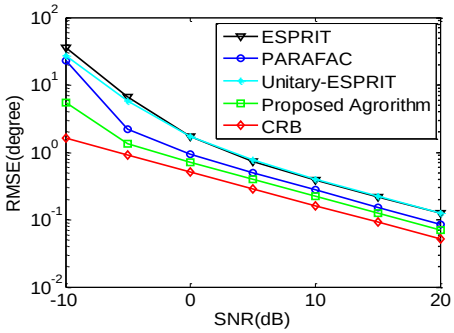

Fig. 4. RMSE comparison with different SNR

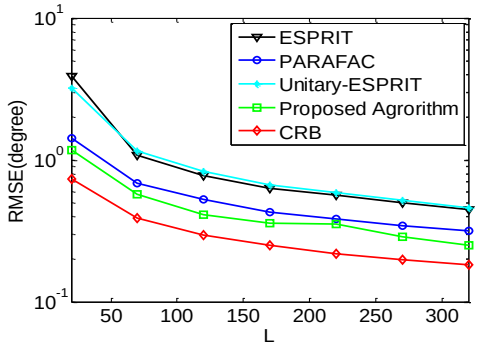

Fig. 5. RMSE comparison with different L.

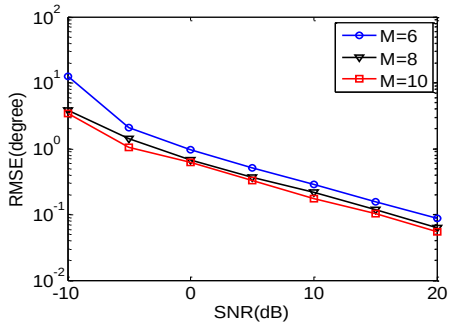

Fig. 6. RMSE performance with different M

The RMSE performance of our algorithm under the condition of different transmit elements number M and different receive antennas number N are investigated separately in the simulation, as shown in Fig. 6 and Fig. 7. $N = 8$, $L = 50$ and $M = 8$, $L = 50$ are considered in Fig. 6

and Fig. 7, respectively. By comparing the above results, one can clearly see that the 2D angle estimation performance of our algorithm is gradually improving with the increasing antenna number. This is commensurate with MIMO systems, as estimation performance can be improved with multiple antennas because of diversity gain.

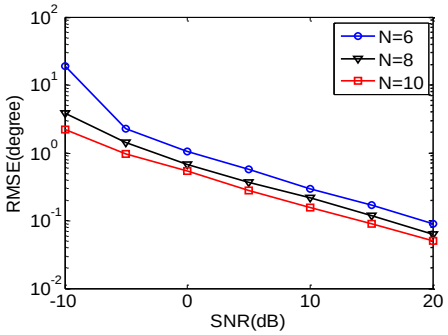

Fig. 7. RMSE performance with different N .

Fig. 8 shows the RMSE performance of our algorithm versus the number of target K , whit $M=8$, $N=7$ and $L=100$. One can see that 2D angle estimation performance of our MCS algorithm degrades with snapshot number L increasing. Fig. 9 presents the RMSE performance of our algorithm with the number of snapshots, with $M=8$, $N=7$. It is clearly shown that 2D angle estimation performance improved in collaboration with L increasing, while our algorithm is effective with small snapshots.

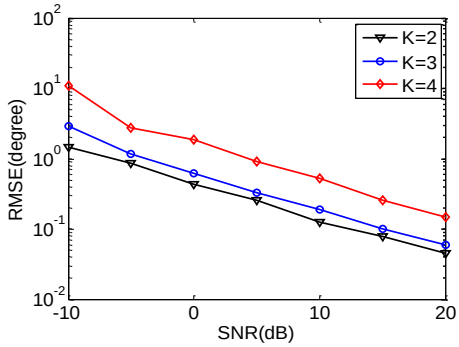

Fig. 8. RMSE performance with different *K*

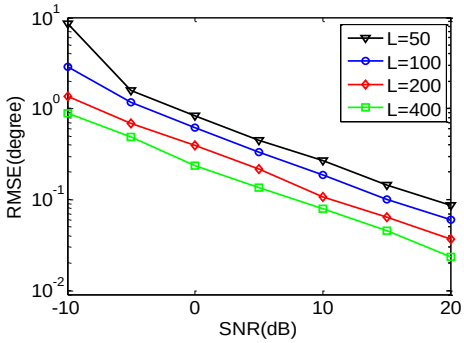

Fig. 9. RMSE performance with different *L*.

VI. Conclusion

An expanded PARAFAC algorithm is developed for 2D angle estimation in monostatic L shape MIMO radar. The virtual aperture of the proposed algorithm is expand with unitary transform, and 2D angle estimation problem in our work was linked to the PARAFAC model. Our algorithm is attractive from the perspective estimation accuracy. It achieves better angle estimation performance to the traditional ESPRIT method and PARAFAC algorithm. Our algorithm doesn't require singular value decomposition of the received data while automatically paired the estimated angles, which means it have blind and robust characteristic. Also, simulation results showed that improvement of the proposed algorithm.

References

[1] E. Fishler, A. Haimovich, R. Blum, *et al*., "MIMO radar: an idea whose time has come," in *Proc. IEEE Radar Conf*., April 2004, pp. 71-78

[2] A. M. Haimovich, R. S. Blum, and L. J. Cimini, "MIMO radar with widely separated antennas," *IEEE Signal Process Mag*., vol. 25, no. 1, pp. 116-129, 2008.

[3] J. Lee, S. Jeong, G. Park, *et al*., "Performance analysis of natural frequency-based multiple radar target recognition for multiple-input-multiple-output radar application," *IET Radar Sonar Navig*., vol. 8, no. 5, pp. 457-464, 2014.

[4] J. He, D. Feng, and L. Ma, "Reduced-dimension clutter suppression method for airborne multiple-input multiple-output radar based on three iterations," *IET Radar Sonar Navig*., vol. 9, no. 3, pp. 249-254, 2015.

[5] X. Zhang, Y. Huang, C. Chen, *et al*., "Reduced-complexity Capon for direction of arrival estimation in a monostatic multiple-input multiple-output radar," *IET Radar Sonar Navig*., vol. 6, no. 8, pp. 796-801, 2012.

[6] H. Yan, J. Li, and G. Liao, "Multitarget identification and localization using bistatic MIMO radar systems," *EURASIP J. Adv. Signal Process.*, vol. 2008, vol. 1, no. 1, p. 1, 2007.

[7] C. Duofang, C. Baixiao, and Q. Guodong, "Angle estimation using ESPRIT in MIMO radar," *Electron. Lett.*, vol. 44, no. 12, pp.770-771, 2008.

[8] C. Jinli, G. Hong, and S. Weimin, "Angle estimation using ESPRIT without pairing in MIMO radar," *Electron. Lett.*, vol. 44, no. 24, pp. 1422-1423, 2008.

[9] Z. D. Zheng and J. Y. Zhang, "Fast method for multi-target localisation in bistatic MIMO radar," *Electron. Lett.*, vol. 47, no. 2, pp. 138-139, 2011.

[10] X. Zhang, Z. Xu, L. Xu, and D. Xu, "Trilinear decomposition-based transmit angle and receive angle estimation for multiple-input multiple-output radar," *IET Radar Sonar Navig*., vol. 5, no. 6, pp. 626-631, 2011.

[11] J. Li and M. Zhou, "Improved trilinear decomposition-based method for angle estimation in multiple-input multiple-output radar," *IET Radar Sonar Navig*., vol. 7, no. 9, pp. 1019-1026, 2013.

[12] J. B. Kruskal, "Three-way arrays: rank and uniqueness of trilinear decompositions, with application to arithmetic complexity and statistics," *Linear Algebra and its Applications*, vol. 18, no. 2, pp. 95-138, 1977.
[13] D. Nion and N. D. Sidiropoulos, "Adaptive algorithms to track the PARAFAC decomposition of a third-order tensor," *IEEE Trans. Signal Process*., vol. 57, no. 6, pp. 2299-2310, 2009.
[14] N. D. Sidiropoulos and A. Kyrillidis, "Multi-way compressed sensing for sparse low-rank tensors," *IEEE Signal Process. Lett*., vol. 19, no. 11, pp. 757-760, 2012.
[15] R. Cao, X. Zhang, and W. Chen, "Compressed sensing parallel factor analysis-based joint angle and Doppler frequency estimation for monostatic multiple-input–multiple-output radar," *IET Radar Sonar Navig*., vol. 8, no. 6, pp. 597-606, 2014.
[16] D. Nion and N. D. Sidiropoulos, "A PARAFAC-based technique for detection and localization of multiple targets in a MIMO radar system," in *Proc. IEEE Int. Conf. Acoustics, Speech and Signal Processing*, April 2009, pp. 2077-2080
[17] S. Kareemulla and V. Kumar, "A novel compact MIMO antenna for ultra wideband applications," in *Proc. IEEE Int. Conf. Signal Process., Info. Com. Energy Sys.*, Feb. 2015, pp. 1-5
[18] F. Wen and G. Zhang, "Two-dimensional direction-of-arrival estimation for trilinear decomposition-based monostatic cross MIMO radar," *Math. Prob. Eng.*, 2013.
[19] R. Xie, Z. Liu, and Y. Liu, "Multi-target identification and localization in MIMO radar with L-shape arrays," *Sys. Eng. Ele.*, vol. 32, no. 1, pp. 49-52, 2010.
[20] J. Li and X. Zhang, "Unitary reduced-dimensional estimation of signal parameters via rotational invariance techniques for angle estimation in monostatic multiple-input–multiple-output radar with rectangular arrays," *IET Radar Sonar Navig*., vol. 8, no. 6, pp. 575-584, 2014.
[21] Y. Hua, T. K. Sarkar, and D. D. Weiner, "An L-shaped array for estimating 2-D directions of wave arrival," *IEEE Trans. Antennas Propagation*, vol. 39, no. 2, pp. 143-146, 1991.
[22] I. Bekkerman and J. Tabrikian, "Target detection and localization using MIMO radars and sonars," *IEEE Trans. Signal Process*., vol. 54, no. 10, pp. 3873-3883, 2006.
[23] M. Haardt and J. A. Nossek, "Unitary ESPRIT: How to obtain increased estimation accuracy with a reduced computational burden," *IEEE Trans. Signal Process*., vol. 43, no. 5, pp. 1232-1242, 1995.
[24] T. Jiang and N. D. Sidiropoulos, "Kruskal's permutation lemma and the identification of CANDECOMP/PARAFAC and bilinear models with constant modulus constraints," *IEEE Trans. Signal Process*., vol. 52, no. 9, pp. 2625-2636, 2004.
[25] J. B. Kruskal, "Three-way arrays: rank and uniqueness of trilinear decompositions, with application to arithmetic complexity and statistics," *Linear Algebr. Appl*., vol. 18, pp. 95-138, 1977.
[26] P. Stoica and A. Nehorai, "Performance study of conditional and unconditional direction-of-arrival estimation," *IEEE Trans. Signal Process*., vol. 38, no. 10, pp. 1783-1795, 1990.

Dongmei Huang was born in Jiangsu Province, China, in 1986. She received the B.S. degree from the Naval Command College, Nanjing, in 2010 and the M.S. degree from the Nanjing University of Aeronautics and Astronautics, China, in 2015. She is currently a lecture in Naval Command College. Her research interests include array signal processing, radar signal processing and tensor signal processing.

Jian-Zhong Xu was bone in Jiangsu Province, China, in 1965, He is currently a researcher in Naval Command College. His research interests include array signal processing, compressive sensing and image signal processing.

Ding Li was bone in Jiangsu Province, China, in 1985. He is currently a lecture in Naval Command College. Her research interests include radar signal processing, image signal processing.